

# Diffusion through Reversibly Associating Polymer Networks

Helen Park, 2008

Advised by Mitchell Anthamatten, Ph.D.

Department of Chemical Engineering

Many natural macromolecules, like proteins and DNA, are equipped with site-specific, non-covalent molecular interactions. These interactions lead to intricate secondary structures such as the double helix, self-assembled phospholipid membrane bilayers, and precisely folded protein structures that are vital to life and rely on non-covalent interactions to “guide” molecular organization. Mankind has begun to borrow such concepts from nature to engineer responsive materials. In recent years, for example, the use of strong, highly directional hydrogen bonds has enabled polymers with temperature-tunable architectures to be engineered.<sup>1,2</sup> Site-specific hydrogen bonding and ionic interactions in solution can lead to aggregation, gelation, or sudden viscosity changes that are triggered by slight changes in polymer concentration, pH, or temperature.<sup>3-5</sup> In the melt, rigid and elastic polymer networks can be reversibly transformed into a low viscosity polymer melt simply by heating. This new materials concept is playing an important role in the development of recyclable (thermoplastic) elastomers.<sup>6-8</sup>

The quest to fully understand structure-property relationships of polymers decorated with hydrogen bonding groups has opened a new field at the interface of polymers and supramolecular chemistry. Our laboratory has synthesized novel polymer networks which contain both covalent crosslinks and non-covalent crosslinks (Figure 1). Non-covalent crosslinks arise from the presence of ureidopyrimidone (UPy) side-groups, which are well known to undergo strong, yet reversible, H-bond association.<sup>9,10</sup> At low temperatures, the rate of H-bond dissociation is slow, and the material behaves as if it is

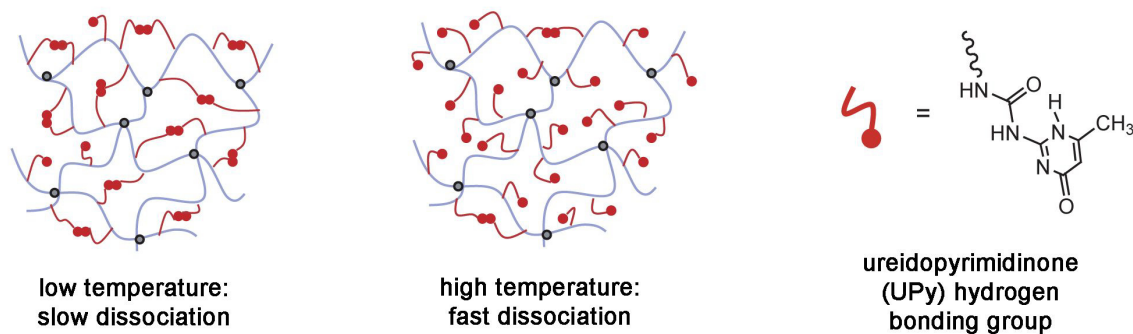
highly crosslinked—like a rigid solid. At higher temperatures, H-bond dissociation is fast, and the material behaves as if it only contains covalent crosslinks—like a soft elastomer. Consequently, mechanical properties show unusual temperature dependence. Shape-memory responses of these and similar networks have been carefully studied.<sup>11,12</sup>

While a great deal of research has focused on controlling polymer rheological properties, to our knowledge no studies have examined how reversible association affects molecular transport. The primary goal of our research is to determine how the rate of molecular transport across dynamic hydrogen bonded networks depends on temperature. We hypothesize that the presence of long-lived hydrogen-bonds will decrease the rate of molecular transport at lower temperatures. A secondary question we raise is how the molecular size of the penetrants influences molecular diffusion. To address this issue, molecular transport of ethanol across polymer networks is compared to that of a much larger organic dye.

## Experimental Approach

Dynamic networks were synthesized using free radical polymerization of butyl acrylate (BA), a crosslinker (trimethylolpropane trimethacrylate, TMP-TMA), and a UPy-functionalized acrylate monomer. Details of chemical synthesis are described elsewhere.<sup>11</sup> The current study focuses on two samples: a network containing only covalent crosslinks, **NW**, and a dynamic network, **DNW** which is composed of a small fraction (2 wt %) of UPy-functionalized monomer. Sample

**Figure 1:** Cartoon depicting architecture of dynamic networks at low and high temperature. Molecular transport through networks is hypothesized to depend strongly on temperature.



Sample	BA (backbone monomer)	TMP-TMA (covalent crosslinker)	UPy-acrylate (reversible crosslinker)
NW	98.5	1.5	0
DNW	96.5	1.5	2

**Table 1:** Composition of dynamic networks; all values are on a mol % basis.

compositions are summarized in Table 1.

To study molecular transport through synthesized networks, sorption-desorption (S-D) and resorption-redesorption (RS-DS) of ethanol were performed on networks with and without UPy side-groups. Experiments were repeated at several different temperatures ranging from 20 to 60 °C. Dry samples containing UPy side-groups were swollen in ethanol. Samples were periodically wiped dry and weighed to determine the amount of ethanol uptake. This procedure was repeated until the network polymers were saturated with ethanol. Desorption and redesorption were performed under a dry nitrogen blanket until the sorbed ethanol was fully removed. For polymers not containing UPy side-groups, data were acquired only up to 50 °C, because these networks started to fracture at higher temperatures.

To study mass transport of larger molecular penetrants through dynamic networks, permeation studies were conducted. Ethanol-swollen polymer networks, ~1 mm thick, were placed between two water-jacketed, temperature-controlled glass chambers. Initially, chamber A was filled with a dye solution [0.1 mM 4-(Dicyanomethylene)-2-t-butyl-6-(1,1,7,7-tetramethyljulolidyl-9-enyl)-4H-pyran, DCJTb,  $M_n = 453.6$  g/mol] in ethanol, and chamber B was filled with pure ethanol. Both chambers were well stirred, and the amount of dye in chamber B was measured with a custom-built photo-detector. Runs were repeated for several different temperatures ranging from 20 to 60 °C. A drawing of the experimental apparatus is

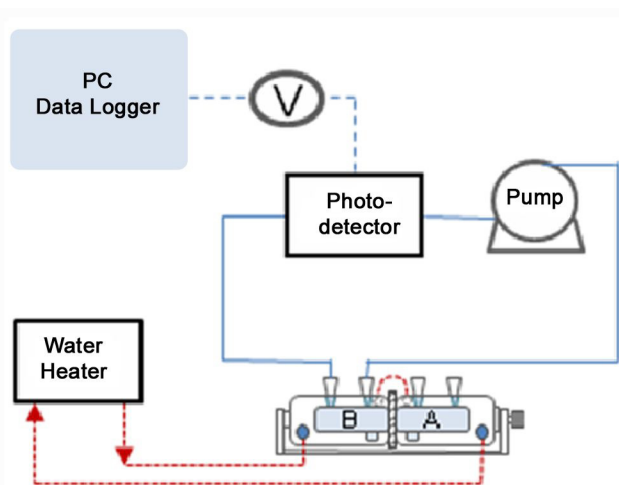


**Figure 2:** Experimental apparatus used to study dye diffusion across solvent-swollen, dynamic polymer networks.

shown in Figure 2.

## Results and Discussion

**Solvent Sorption.** Ethanol sorption data acquired at different temperatures are shown in Figure 3 where ethanol uptake ( $Q_t$ ) is defined as

$$Q_t = \frac{\text{mass of EtOH sorbed} / M_w \text{ of EtOH}}{\text{mass of polymer}} \times 100. \quad [1]$$

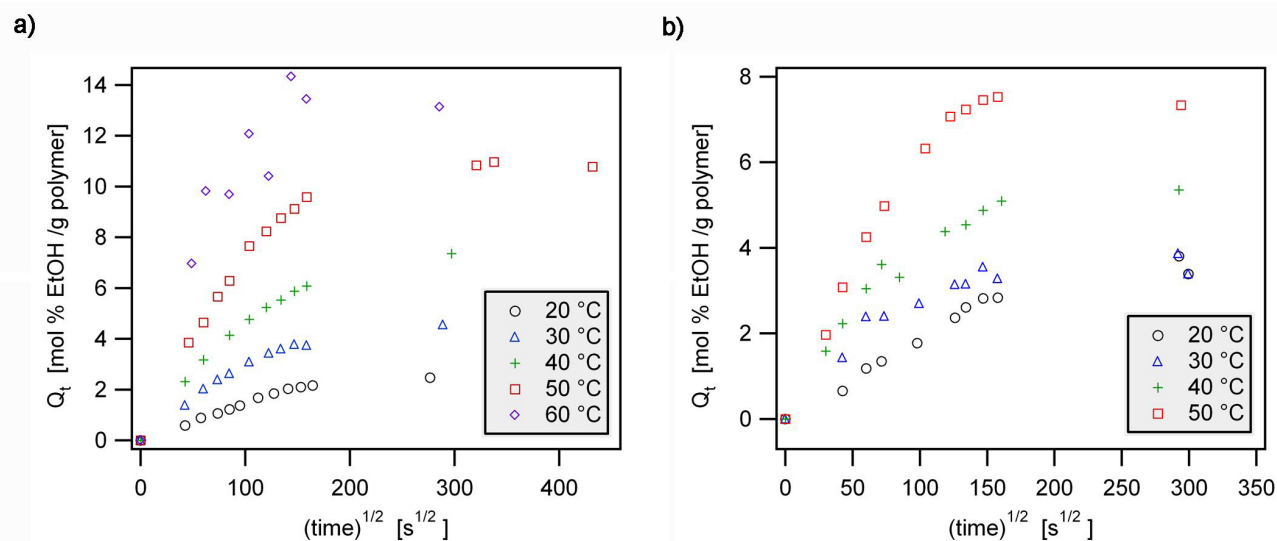
With increasing time, samples become saturated with ethanol, and  $Q_t$  approaches an equilibrium value of  $Q_\infty$ .

At short times, data are nearly linear, and, in this regime, the diffusion coefficient of ethanol  $D_{Et}$  describing transport into the network polymers can be determined from mass-uptake data<sup>13</sup> by

$$D_{Et} = \pi \left[ \frac{h\theta}{4Q_\infty} \right]^2 \quad [2]$$

where  $h$  is the initial thickness of the polymer,  $\theta$  is the slope of a plot of  $Q_t$  vs.  $t^{1/2}$  (at short times), and  $Q_\infty$  is the fractional

**Figure 3:** Ethanol uptake curves for a) UPy-functionalized networks (DNW) and b) unfunctionalized networks (NW). Measured values of ethanol uptake ( $Q_t$ ) are plotted versus  $t^{1/2}$  for different temperatures.



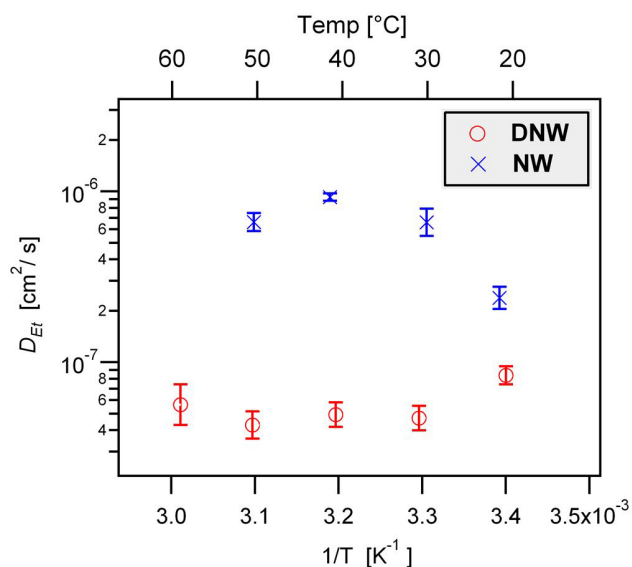


**Figure 4:** Temperature dependence of ethanol diffusivity ( $D_{Et}$ ) through UPy-functionalized networks (DNW) and unfunctionalized networks (NW). Error bars were determined by “propagation of error” analysis.

uptake of solvent at infinite time. Diffusion coefficients were measured at several different temperatures, and results are summarized in Figure 4. Measured values of  $D_{Et}$  through conventional networks (NW) are on the order of  $1 \times 10^{-6}$   $\text{cm}^2/\text{s}$ . These values are on the same scale as the diffusion coefficients of linear alkanes measured through styrene-butadiene crosslinked rubber membranes.<sup>14</sup> Interestingly, diffusion of ethanol into functionalized, dynamic networks (DNW) is about an order of magnitude slower than diffusion into conventional networks (NW). This suggests that either the presence of UPy groups, or the presence of additional, hydrogen-bonded crosslinks, interferes with mass transport.

Figure 4 also shows that mass transport of ethanol into the network polymers depends weakly, if at all, on temperature. This is a little surprising because other studies of penetrant diffusion through crosslinked networks<sup>14,15</sup> show diffusion to be thermally-activated, i.e., faster diffusion occurs at higher temperatures. However, these studies all involved penetrant molecules that are much larger than ethanol. The lack of temperature dependence in Figure 4 suggests that ethanol transport is determined by solvent-polymer interactions, and not by the

presence of crosslinks. Obstruction-scaling models support this view and show that network obstructions become less important when penetrant molecules are smaller than the characteristic length scale of the network mesh.<sup>16,17</sup>

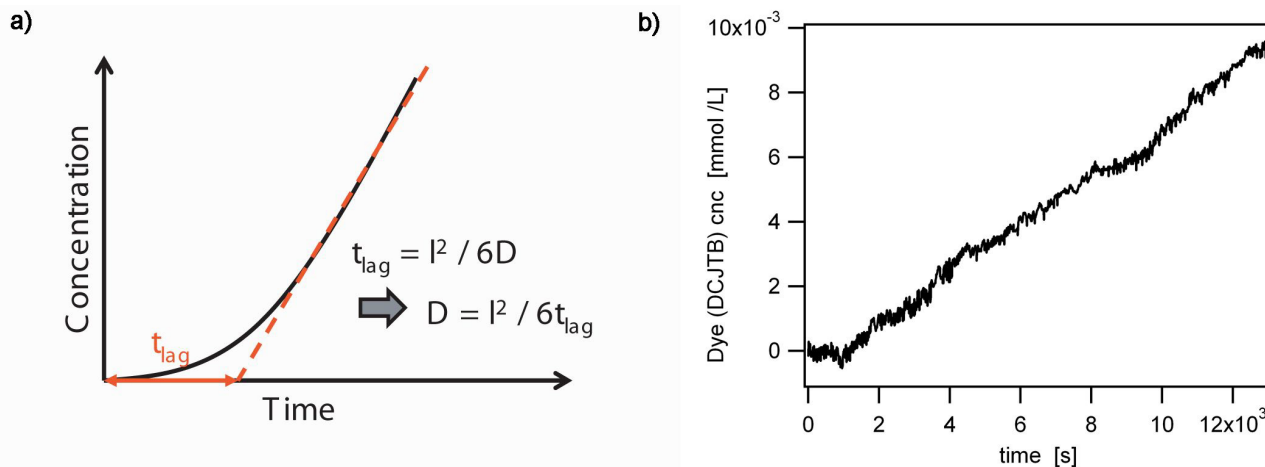
**Permeation Studies.** To examine transport of larger molecules through dynamic networks, permeation experiments were performed using a large dye molecule (DCJTB,  $M_n = 453.6$  g/mol). Diffusion coefficients for DCJTB ( $D_{Dye}$ ) through synthesized networks were determined by using the time-lag method.<sup>18</sup> This method assumes that both chambers are well-mixed and that solute is only initially present in chamber A (See Figure 2). Briefly, the cumulative amount of solute transferred through the membrane  $Q_t$ , is related to the diffusion coefficient by

$$Q_t = V_{B0} C_B(t) = \frac{A_x D_{dye} C_{A0}}{l} \left( t - \frac{l^2}{6D_{dye}} \right) \quad [3]$$

where  $V_{B0}$  is the initial volume of chamber B,  $C_B(t)$  is the dye concentration in chamber B,  $A_x$  is the membrane cross-sectional area,  $C_{A0}$  is the initial dye concentration in chamber A, and  $l$  is the membrane thickness. Figure 5b shows a typical plot of experimental data in the form of concentration vs. time. Diffusion coefficients,  $D_{Dye}$ , were determined from the x-intercept of a tangential line fit to experimental data, also known as the “time lag” ( $t_{lag} = l^2/6D_{Dye}$ ). For each run, the membrane thickness was measured in the dry state, and the ethanol-swollen membrane thickness,  $l$ , was estimated using results of ethanol solvent-sorption studies.

Measured diffusion coefficients of dye diffusing through UPy functionalized networks (DNW) are summarized in Figure 6. The rate of dye transport increases with increasing temperature and exhibits much greater temperature dependence compared to that of ethanol. The activation energy for diffusive transport was 42.3 kJ/mol based on the slope of the best-fit line to  $D_{Dye}$  versus  $1/T$ . This activation energy is significantly higher than the activation energy of linear alkanes diffusing through traditional, styrene-butadiene crosslinked networks ( $\sim 20$  kJ/mol).<sup>14</sup> Interestingly, the measured activation energy is more comparable to the energy barrier of UPy dimer dissociation of 70 kJ/mol<sup>19</sup> (measured in  $\text{CHCl}_3$ ). This suggests that dye transport through reversibly associating polymer net-

**Figure 5:** Overview of time-lag method: a) schematic showing how permeation data are analyzed to determine molecular diffusivity, b) typical experimental data acquired on a dynamic network membrane. The time-lag is defined as the x-intercept of a linear fit to data at later times.



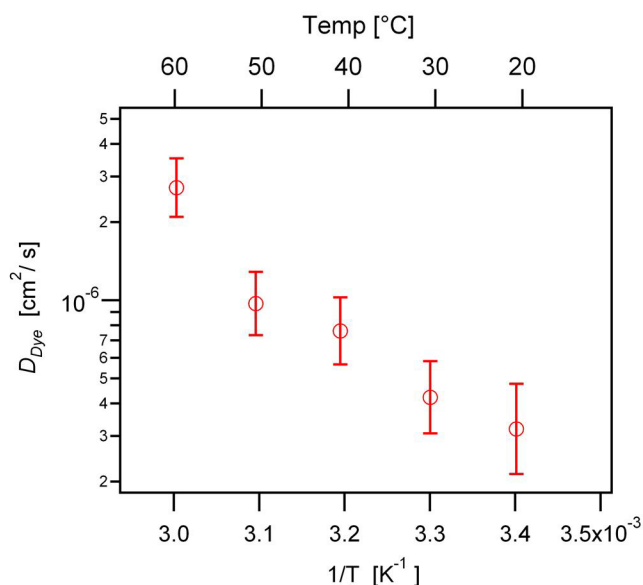


**Figure 6:** Temperature dependence of dye diffusivity through UPy-functionalized networks (DNW). Error bars were determined by “propagation of error” analysis.

works may be controlled by the rate of H-bond dissociation. At low temperatures, H-bond dissociation is believed to reduce mobility and interfere with mass transport of dye through the functionalized polymer. At high temperatures, the rate of dissociation is so fast that dynamic crosslinks do not interfere with transport.

## Conclusions

Solvent sorption and permeation experiments were conducted to assess how molecular diffusion through dynamic networks depends on temperature and on molecular size. Ethanol diffusion through networks with and without UPy (hydrogen bonding) side-groups showed little, if any, temperature dependence. On the other hand, mass transport of a larger molecule (a dye, DCJTb) through networks containing UPy side-groups is clearly a thermally-activated process. The activation energy for this process is about 45 kJ/mol and is comparable to the activation energy of H-bond dissociation (of UPy side-groups). Therefore, experiments support the notion that mass transport may be limited by the rate of dissociation of hydrogen bonded side-groups. However, to confirm this hypothesis, more studies need to be conducted.

Further development of polymers with temperature-sensitive permeabilities may result in important applications. Transdermal medicine patches, for example, are envisioned to target the drug delivery to infected areas of wounds, assuming that infected tissue has a slightly higher temperature than healthy tissue. Another potential application is that of the “smart” labels, which are able to track the temperature-exposure of perishable goods through the diffusion of a dye.

## Acknowledgement

This project was funded by Professor Richard Eisenberg and by the Department of Chemical Engineering, University of Rochester. The author acknowledges Andrew Hilmer for providing Figure 2.

## Appendix

### Calculation of Error Bars for Sorption Experiment

For the error analysis of the diffusion coefficients of the sorption experiments, propagation of error was used to determine the error bars. First, some of the basic formulas of propagation of error will be discussed. For expressions of  $Z$  representative of  $Z=A\pm B$ , the error,  $\Delta Z$ , is calculated as:

$$\Delta Z = \sqrt{(\Delta A)^2 + (\Delta B)^2} \quad [A1]$$

For expressions of  $Z$  representative of  $Z=AxB$  or  $Z=A/B$  the error,  $\Delta Z$ , is calculated as:

$$\Delta Z = Z \sqrt{\left(\frac{\Delta A}{A}\right)^2 + \left(\frac{\Delta B}{B}\right)^2} \quad [A2]$$

For expressions of  $Z$  representative of  $Z = \ln A$ , the error,  $\Delta Z$ , is calculated as:

$$\Delta Z = \frac{\Delta A}{A} \quad [A3]$$

Next, diffusion coefficients are determined by equation [2] for solvent sorption. The error in polymer thickness,  $\Delta h$ , was determined by making 10 random measurements of a polymer and using the standard deviation of the measurements as the error of polymer thickness. The error in the slope of plot  $Q_t$  vs.  $t^{1/2}$ ,  $\Delta \theta$ , was determined by using the LINEST function in Excel. Since the molar uptake of solvent/g of polymer,  $Q_\infty$ , was experimentally determined by:

$$Q_t = \frac{(m_{p+EtOH} - m_p) M_w}{m_p} \times 100 = \frac{m_{EtOH} / M_w}{m_p} \times 100 \quad [A4]$$

where  $m_{p+EtOH}$  is the mass of polymer with the sorbed ethanol,  $m_{EtOH}$  is the mass of the sorbed ethanol,  $m_p$  is the mass of the dry polymer, and  $M_w$  is the molecular weight of ethanol,  $m_{EtOH} = m_{p+EtOH} - m_p$ . Knowing the two errors,  $\Delta m_{p+EtOH}$  and  $\Delta m_p$ , which are estimated to be about 0.0001 g, the error,  $\Delta m_{EtOH}$  can be determined by:

$$\Delta m_{EtOH} = \sqrt{(\Delta m_{p+EtOH})^2 + (\Delta m_p)^2} \quad [A5]$$

From  $\Delta m_{EtOH}$  and equation [A5], the error of  $Q_\infty$  is determined by:

$$\Delta Q_\infty = Q_\infty \sqrt{\left(\frac{\Delta m_{EtOH}}{m_{EtOH}}\right)^2 + \left(\frac{\Delta m_p}{m_p}\right)^2} \quad [A6]$$

Similarly, the error of  $(h\theta)$ , can be determined by:

$$\Delta(h\theta) = (h\theta) \sqrt{\left(\frac{\Delta h}{h}\right)^2 + \left(\frac{\Delta \theta}{\theta}\right)^2} \quad [A7]$$

Subsequently, the error of  $(h\theta/Q_\infty)$  is determined by:

$$\Delta\left(\frac{h\theta}{Q_\infty}\right) = \left(\frac{h\theta}{Q_\infty}\right) \sqrt{\left(\frac{\Delta(h\theta)}{h\theta}\right)^2 + \left(\frac{\Delta Q_\infty}{Q_\infty}\right)^2} \quad [A8]$$

Therefore, the error of  $D$  is determined by the expression:

$$\Delta D = D \sqrt{\left(\frac{\Delta\left(\frac{h\theta}{Q_\infty}\right)}{\left(\frac{h\theta}{Q_\infty}\right)}\right)^2 + \left(\frac{\Delta\left(\frac{h\theta}{Q_\infty}\right)}{\left(\frac{h\theta}{Q_\infty}\right)}\right)^2} = D\sqrt{2} \frac{\Delta\left(\frac{h\theta}{Q_\infty}\right)}{\left(\frac{h\theta}{Q_\infty}\right)} \quad [\text{A9}]$$

This leads to the error used for the error bars:

$$\Delta(\ln D) = \frac{\Delta D}{D} \quad [\text{A10}]$$

### Calculation of Error Bars for Permeation Experiment

For the error analysis of the diffusion coefficients of the permeation studies, propagation of error was also used to determine the error bars, and the same basic formulas discussed in Appendix A were used. The diffusion coefficients of the permeation studies were determined by the time-lag expression. The error of thickness of polymer,  $\Delta l$ , was determined by the same method for the  $\Delta b$  discussed in Appendix A. Therefore,

$$\Delta(t^2) = (t^2) \sqrt{\left(\frac{\Delta l}{l}\right)^2 + \left(\frac{\Delta l}{l}\right)^2} = (t^2) \sqrt{2} \frac{\Delta l}{l} \quad [\text{A11}]$$

The tangential straight line which was added to the plot of concentration vs. time can be expressed as  $y=mx+b$ , where  $y$  is the concentration and  $x$  is time. Then  $\Delta t_{lag} = -b/m$ , and

$$\Delta(t_{lag}) = (t_{lag}) \sqrt{\left(\frac{\Delta b}{b}\right)^2 + \left(\frac{\Delta m}{m}\right)^2} \quad [\text{A12}]$$

Therefore, the error of  $D$  is determined by the expression:

$$\Delta D = D \sqrt{\left(\frac{\Delta l^2}{l^2}\right)^2 + \left(\frac{\Delta t_{lag}}{t_{lag}}\right)^2} \quad [\text{A13}]$$

This leads to the error used for the error bars:

$$\Delta(\ln D) = \frac{\Delta D}{D} \quad [\text{A14}]$$

### References

1. Brunsveld, L.; Folmer, B. J. B.; Meijer, E. W.; Sijbesma, R. P. *Chemical Reviews* 2001, 101, (12), 4071-4097.
2. Sherrington, D. C.; Taskinen, K. A. *Chemical Society Reviews* 2001, 30, (2), 83-93.
3. Chassenieux, C.; Nicolai, T.; Tassin, J. F.; Durand, D.; Gohy, J. F.; Jerome, R. *Macromolecular Rapid Communications* 2001, 22, (15), 1216-1232.
4. Klier, J.; Scranton, A. B.; Peppas, N. A. *Macromolecules* 1990, 23, (23), 4944-4949.
5. Sivakova, S.; Bohnsack, D. A.; Mackay, M. E.; Suwanmala, P.; Rowan, S. J. *J. Am. Chem. Soc.* 2005, 127, 18202-18211.
6. Rieth, L. R.; Eaton, R. F.; Coates, G. W. *Angewandte Chemie-International Edition* 2001, 40, (11), 2153-2156.
7. Chino, K.; Ashiura, M. *Macromolecules* 2001, 34, (26), 9201-9204.
8. Kautz, H.; van Beek, D. J. M.; Sijbesma, R. P.; Meijer, E. W. *Macromolecules* 2006, 39, (13), 4265-4267.
9. Sijbesma, R. P.; Beijer, F. H.; Brunsveld, L.; Folmer, B. J. B.; Hirschberg, J. H. K. K.; Lange, R. F. M.; Lowe, J. K. L.; Meijer, E. W. *Science* 1997, 278, (5343), 1601-1604.
10. Hirschberg, J. H. K. K.; Beijer, F. H.; van Aert, H. A.; Magusim, P. C. M. M.; Sijbesma, R. P.; Meijer, E. W. *Macromolecules* 1999, 32, (8), 2696-2705.
11. Li, J.; Viveros, J. A.; Wrue, M. H.; Anthamatten, M. *Advanced Materials* 2007, 19, 2851-2855.
12. Cao, Y.; Guan, Y.; Du, J.; Luo, J.; Peng, Y.; Yip, C. W.; Chan, A. S. C. *J. Mater. Chem.* 2002, 12, 2957.
13. Crank, J., *The Mathematics of Diffusion*. 2nd ed.; Oxford University

Press: London, 1975.

14. George, S. C.; Knorren, M.; Thomas, S. *Journal of Membrane Science* 1999, 163, (1), 1-17.
15. Gao, Z.; Pilar, J.; Schlick, S. *Journal of Physical Chemistry* 1996, 100, (20), 8430-8435.
16. Zhang, Y.; Amsden, B. G. *Macromolecules* 2006, 39, (3), 1073-1078.
17. Amsden, B.; Grotheer, K.; Angl, D. *Macromolecules* 2002, 35, (8), 3179-3183.
18. Zhang, W.; Furusaki, S. *Biochemical Engineering Journal* 2001, 9, (1), 73-82.
19. Soentjens, S. H. M.; Sijbesma, R. P.; van Genderen, M. H. P.; Meijer, E. W. *J. Am. Chem. Soc.* 2000, 122, 7487-7495.